WAVE PACKET DYNAMICS AND CONTROL IN EXCITED STATES OF MOLECULAR NITROGEN

Mizuho Fushitani,[1,*] Hikaru Fujise,[2] Akiyoshi Hishikawa,[1,2] Daehyun You,[3] Shu Saito,[3] Yu Luo,[3] Kiyoshi Ueda,[3,4,*] Heide Ibrahim,[5] Francois Légaré,[5] Stephen T. Pratt,[6,*] Per Eng-Johnsson,[7] Johan Mauritsson,[7] Anna Olofsson,[7] Jasper Peschel,[7] Emma R. Simpson,[7] Paolo Antonio Carpeggiani,[8] Dominik Ertel,[9] Praveen Kumar Maroju,[9] Matteo Moioli,[9] Giuseppe Sansone,[9] Ronak Shah,[9] Tamás Csizmadia,[10] Mathieu Dumergue,[10] N. G. Harshitha,[10] Sergei Kühn,[10] Carlo Callegari,[11] Miltcho Danailov,[11] Alexander Demidovich,[11] Lorenzo Raimondi,[11] Marco Zangrando,[11,12] Giovanni De Ninno,[11,13] Michele Di Fraia,[11] Luca Giannessi,[11, 14] Oksana Plekan,[11] Primoz Rebernik Ribic,[11,13] and Kevin C. Prince[11,15,*]

1. Department of Chemistry, Nagoya University, Furo-cho, Chikusa, Nagoya, Aichi 464-8602, Japan
2. Research Center for Materials Science, Nagoya University, Furo-cho, Chikusa, Nagoya, Aichi 464-8602, Japan
3. Institute of Multidisciplinary Research for Advanced Materials, Tohoku University, Sendai, Miyagi 980-8577, Japan
4. Current addresses: Department of Chemistry, Tohoku University, Sendai 980-8578, Japan, and School Physical Science and Technology, ShanghaiTech University, Shanghai 201210, China
5. INRS, Énergie, Matériaux et Télécommunications, 1650 Bld. Lionel Boulet, Varennes, Québec, J3X 1S2, Canada
6. Chemical Sciences and Engineering Division, Argonne National Laboratory, Lemont, IL 60439 USA
7. Lund University, Department of Physics, Lund, Sweden
8. Technische Universität Wien, Institut für Photonik, Gußhausstraße 27-29, 1040 Wien Austria
9. Stefan-Albert-Ludwigs-Universität Freiburg, Stefan-Meier-Strasse 19, 79104 Freiburg, Germany

10. ELI ALPS, ELI-HU Non-Profit Ltd., Wolfgang Sandner utca 3, H-6728 Szeged, Hungary
11. Elettra Sincrotrone Trieste, I-34149 Trieste, Italy
12. CNR-IOM, I-34149 Trieste, Italy
13. University of Nova Gorica, Vipavska 13, SI-5000 Nova Gorica, Slovenia
14. INFN Laboratori Nazionali di Frascati, Via E. Fermi 54, 00044 Frascati (Roma)
15. Department of Chemistry and Biotechnology, School of Science, Computing and Engineering Technologies, Swinburne University of Technology, Melbourne, Victoria 3122, Australia

*Corresponding Authors

ABSTRACT

Wave packet interferometry with vacuum ultraviolet light has been used to probe a complex region of the electronic spectrum of molecular nitrogen, N_2. Wave packets of Rydberg and valence states were excited by using double pulses of vacuum ultraviolet (VUV), free-electron-laser (FEL) light. These wave packets were composed of contributions from multiple electronic states with moderate principal quantum number ($n \sim 4 – 9$) and a range of vibrational and rotational quantum numbers. The phase relationship of the two FEL pulses varied in time, but as demonstrated previously, a shot-by-shot analysis allows the spectra to be sorted according to the phase between the two pulses. The wave packets were probed by angle-resolved photoionization using an infrared pulse with a variable delay after the pair of excitation pulses. The photoelectron branching fractions and angular distributions display oscillations that depend on both the time delays and the relative phases of the VUV pulses. The combination of frequency, time delay, and phase selection provides significant control over the ionization process, and ultimately improves the ability to analyze and assign complex molecular spectra.

I. INTRODUCTION

Excitation of a band of states in an atom or molecule by a coherent pulse of radiation produces a superposition of states, or wave packet, that evolves over time.[1,2,3] At least initially, this wave packet is often localized and displays particle-like behavior, for example, as a wave packet of Rydberg states reflecting the motion of the excited electron or as a wave packet of vibrational levels reflecting the motion of the atomic nuclei. Probing the wave packet as a function of the delay after the excitation pulse provides the possibility of following the evolution of the wave packet, that is, the electronic or vibrational motion and its dephasing and decay.

If an atom or molecule is excited by a pair of pulses with a well-defined time delay and phase relationship, the wave packets produced by the two pulses interfere, and this interference can be used to control the excitation and decay processes. This approach is known as wave packet interferometry. The method has its origin in the magnetic resonance studies of Ramsey,[4] but over the past few decades, it has become popular at optical wavelengths as well.[5,6,7,8] Recently, double pulses of attosecond Vacuum Ultraviolet (VUV) light have been created with laboratory sources and used in wave packet interferometry experiments.[9,10,11] Seeded FEL light is naturally coherent, and Wituschek et al.[12,13] have used this property to carry out wave packet interference experiments on noble gas atoms and dimers. Using XUV and soft X-ray FEL radiation, Usenko et al.[14,15] have also demonstrated wave packet interference of Auger electrons. Hikosaka and co-workers[16,17] have used two pulses of partially coherent synchrotron radiation to irradiate noble gases, and interpreted their results in terms of wave packet interference, but this interpretation is disputed.[18,19]

Beyond the ability to observe and characterize wave packet behavior, the two-pulse techniques also offer the ability to control the behavior of atoms and molecules.[20] In particular, by varying the timing and relative phase of the two pulses, the character of the excited state wave packets can be shaped to enhance the desired behavior. Work along these lines has been summarized in a number of reviews, and is illustrated by recent examples.[21,22,23,24] With a few exceptions,[13,15] to date most

work at short wavelengths has been performed on atomic targets. Short wavelengths provide access to highly excited molecular Rydberg states and their dynamics. The competition between different decay channels (internal conversion, intersystem crossing, predissociation, fluorescence, etc.) provides considerable insight into the interplay between nuclear and electronic motion, the breakdown of the Born-Oppenheimer approximation, and the interactions between Rydberg and valence states.

Previously, we have reported a study of the dynamics of a group of nitrogen Rydberg states using time-resolved photoelectron spectroscopy.[25] In these experiments, which complemented the earlier work of Fushitani *et al*.,[26] a single FEL pulse was used to prepare the excited state wave packet, and a time-delayed infrared (IR) pulse was used to photoionize it. The wave packet included contributions from multiple Rydberg states as well as valence states. Photoelectron energy and angular distributions were then measured as a function of the IR delay. The time-dependence of the signal revealed oscillations in both the excited state populations and their angular distributions, providing insight into the interactions among the states making up the wave packet. In the present work, we use wave packet interferometry to further probe these excited states. In particular, the ability to control the relative phase between the two VUV pulses, as well as the coarse delay between these two pulses, and the delay of the IR pulse, provides an additional tool for the characterization of the wave packet using multi-dimensional spectroscopy.

II. EXPERIMENT

The experiment was carried out at the Low-Density Matter end-station[27] of the FERMI Free-Electron Laser. The scheme for generating double pulses was based on that described by Gauthier et al.,[28] and consisted of optical wedges for setting a coarse delay, with a Mach-Zehnder interferometer for setting the fine delay. Other aspects of the set-up were described previously.[25] Briefly, the jet-cooled nitrogen was excited by the VUV pulse pair from the FEL and subsequently ionized by an IR pulse (795 nm, 1.560 eV) after a time delay of -350 to 650 fs with respect to the

first VUV pulse, and the photoelectron spectrum was measured with a Velocity Map Imaging (VMI) spectrometer.[29]

The spectral distribution of the FERMI light pulses (henceforth: optical spectrum) was measured for each shot using the single-shot photon spectrometer of FERMI.[30] A single value of the VUV double pulse delay was used. The system was not sufficiently stable in time to provide phase stability, so the phase was extracted for each individual shot from the optical spectrum, using the method described by Wituschek.[12] Symmetric spectra were assigned to pulses with phase $\phi=0$ or π, according to whether they displayed a central maximum or minimum respectively. Other phase values were obtained by interpolation, according to the position of the maximum with respect to the central wavelength. Note that the optical phase of the IR pulse is not controlled relative to the phases of the VUV pulses. In the present experiments, the central VUV wavelength was 80.656 nm (15.372 eV), with a 0.023 eV pulse bandwidth and 140 fs duration, that is, the same single pulse parameters as in our previous paper.[25] All three pulses were linearly polarized with parallel polarization, and the VMI images were inverted using the BASEX software [31] to yield photoelectron angular distributions. These were analyzed to extract photoelectron spectra and the asymmetry parameters β_2 and β_4, which appear as coefficients in the Legendre polynomials describing the angular distribution.

The optical scheme is shown in Figure 1(a), where we follow the notation of Ohmori et al.[6] The first FEL pulse is labelled the pump pulse, the second is the control pulse, and the IR pulse is the probe pulse. The total delay between the pump and control pulses is denoted $\tau + (\phi/2\pi)T$, where τ and $(\phi/2\pi)T$ are respectively the integer quotient and remainder of the total delay, modulo T, ϕ represents the phase delay between the pulses, $T=\lambda/c$ is the period of the FEL light; for our purposes τ can be considered invariant from shot to shot. With this definition, ϕ controls the interference conditions for the two wave packets. The delay Δt is the time between the pump and IR probe pulses, and the temporal evolution of the photoelectron signals as a function of Δt reflects the dynamics of the interfering wave packet. The dependences on the time delay or the relative

phase of the control VUV pulse provide information on the extent to which the Rydberg wave packet can be controlled.

Figure 1(b) shows a stick representation of the N_2 absorption spectrum in the region around the VUV photon energy, along with the oscillator strengths for the observed transitions. Figure 1(c) shows the pulse scheme superimposed on the potential energy curves of the excited states and first

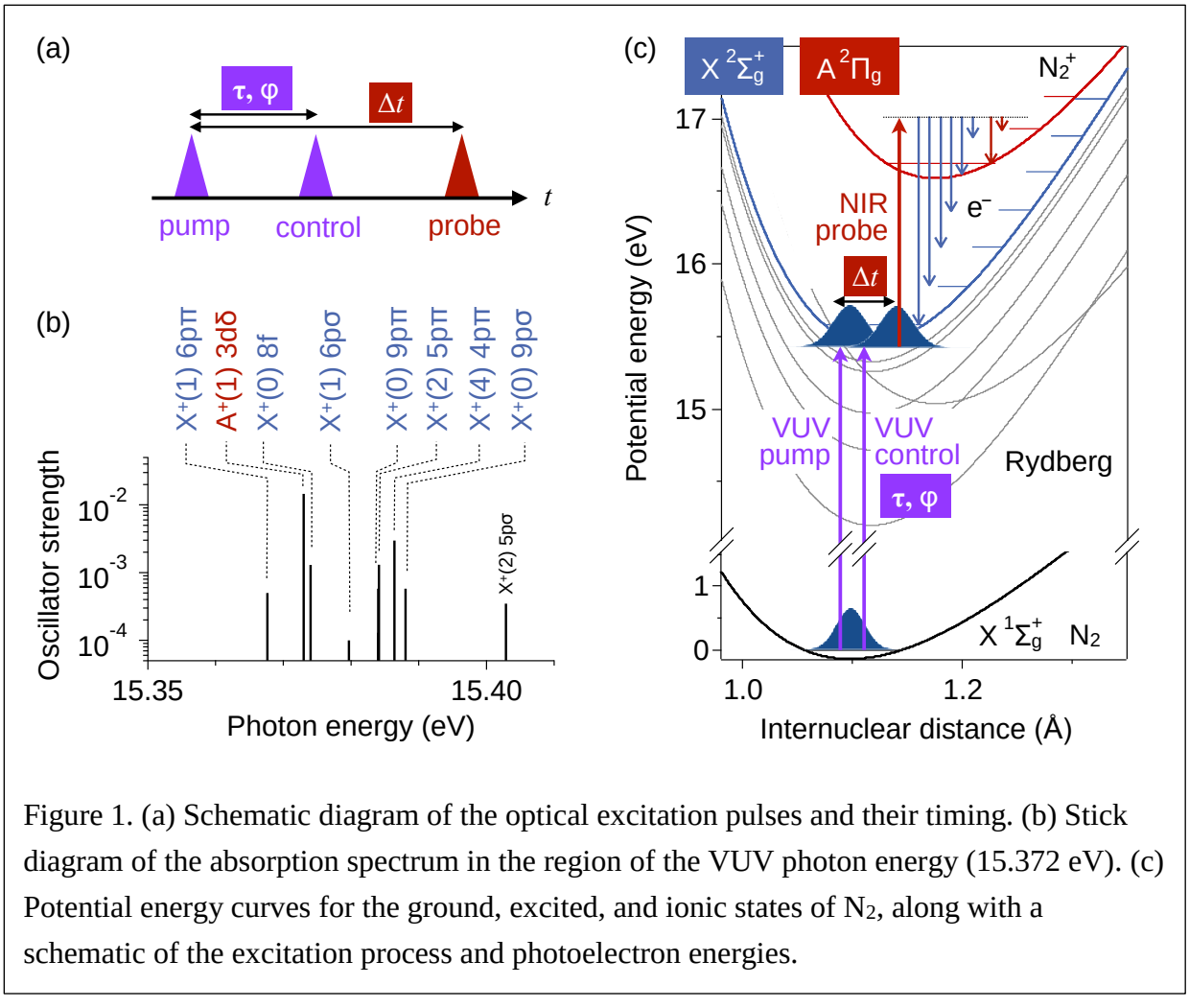

Figure 1. (a) Schematic diagram of the optical excitation pulses and their timing. (b) Stick diagram of the absorption spectrum in the region of the VUV photon energy (15.372 eV). (c) Potential energy curves for the ground, excited, and ionic states of N_2, along with a schematic of the excitation process and photoelectron energies.

ionic state of nitrogen. The excited states are labelled by $\Lambda^+(v)n\ell\lambda$, where Λ^+ (= X^+ or A^+) indicates the electronic state of the ion core, v indicates the vibrational quantum number, n and ℓ the principal quantum number and orbital angular moment of the Rydberg electron, respectively, and

λ the projection of ℓ on the internuclear axis. The photon bandwidth spans transitions to various vibrational levels of four different Rydberg series: $X^+(v)$npσ, $X^+(v)$npπ, $X^+(v)$nf, and $A^+(v)$3dδ.[32,33] In addition, the transition to the b' $^2\Sigma_u^+$, v = 34 level is predicted to lie in this region, but has not been observed. These Rydberg states are strongly coupled to each other, and borrow intensity from the $A^+(1)$3dδ Rydberg state.

The bands in Figure 1(a) are clustered into two groups. The $A^+(1)$3dδ $^1\Pi_u$, $X^+(0)$8f, and $X^+(1)$6pπ bands form the low-energy group centered at ~15.373 eV, while the $X^+(4)$4pπ, $X^+(2)$5pπ, $X^+(0)$9pπ, and $X^+(0)$9pσ bands form the second group at ~15.386 eV. The $X^+(1)$6pσ band appears weakly midway between these two groups.[32] The energy difference between the centers of the two groups of resonances is 13 meV, and a fringe spacing with this value is achieved by a pair of pulses with a delay of 320 fs, suggesting that this would be the best choice for the pump-control delay, τ. Preliminary modelling indicated that a delay of 250 fs would give better contrast, so this value was used. The wave packets made up from the states within the pump and control bandwidths are of rather different character than those in many previous experiments. In particular, the values of the principal quantum number, *n*, are moderate, and the pulse duration is long (or the number of states in the wave packet is small) so that a localized radial wave packet is not created. Similarly, the number of vibrational levels excited in the wave packet is small so that a localized vibrational wave packet is not created. We demonstrate that we can still coherently control the non-localized wave packets, for which the observable photoelectron branching fractions and angular distributions vary with the time delay of the IR probe pulse.

III. RESULTS

Figure 2 shows examples of raw (left side of each panel) and inverted (right side of each panel) VMI images, (a) for phase ϕ=0, and (b) for phase ϕ=π. Each circular line, corresponding to a specific kinetic energy and final state, is clearly visible in both images. The final ionic states are labelled in Fig. 2(a). The pump-control delay was set to a nominal value 250 ± 30 fs as determined

by measuring the cross-correlation signal with the IR pulse. The corresponding optical spectra were Fourier transformed to provide a second determination of the value of the delay as derived from the fringe spacing, yielding a value of $\tau = 250 \pm 7$ fs. The values agree to within the precision with which the delay can be determined by either method. The possible effect of chirp on the pump and control pulses is not discussed here, but it is considered in more detail in a separate publication.[34]

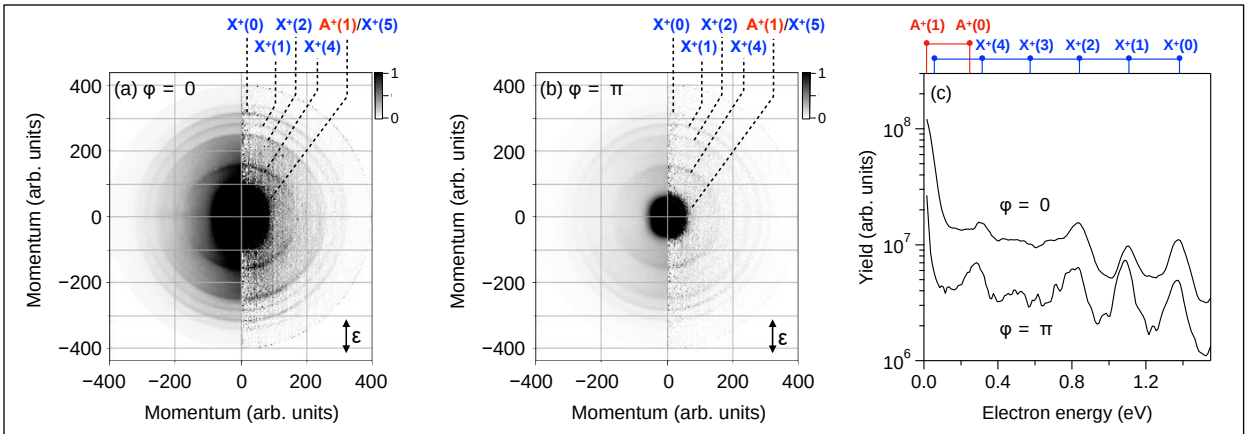

Figure 2. Examples of raw (left side) and inverted (right side) VMI images at τ=250 fs and Δt=550 fs. (a) phase ϕ=0, (b) phase ϕ=π. (c) Photoelectron spectra for ϕ=0 and π.

Figure 3 displays the photoelectron yield and angular asymmetry parameters for phase ϕ = 0. Strong oscillations are visible in the photoelectron yield, Fig. 3(a), especially for the $A^+(1)$, $X^+(4)$ and $X^+(2)$ ionic states (hereafter denoted A1, X4 and X2). Oscillations are also visible in the β_2 parameter for the A1 and X4 states, and in the β_4 parameter for the A1 state. Similar oscillations as a function of probe delay were observed in the branching fractions and angular distributions in the earlier time-resolved photoelectron spectra[25] without the control pulse.

Fig. 3

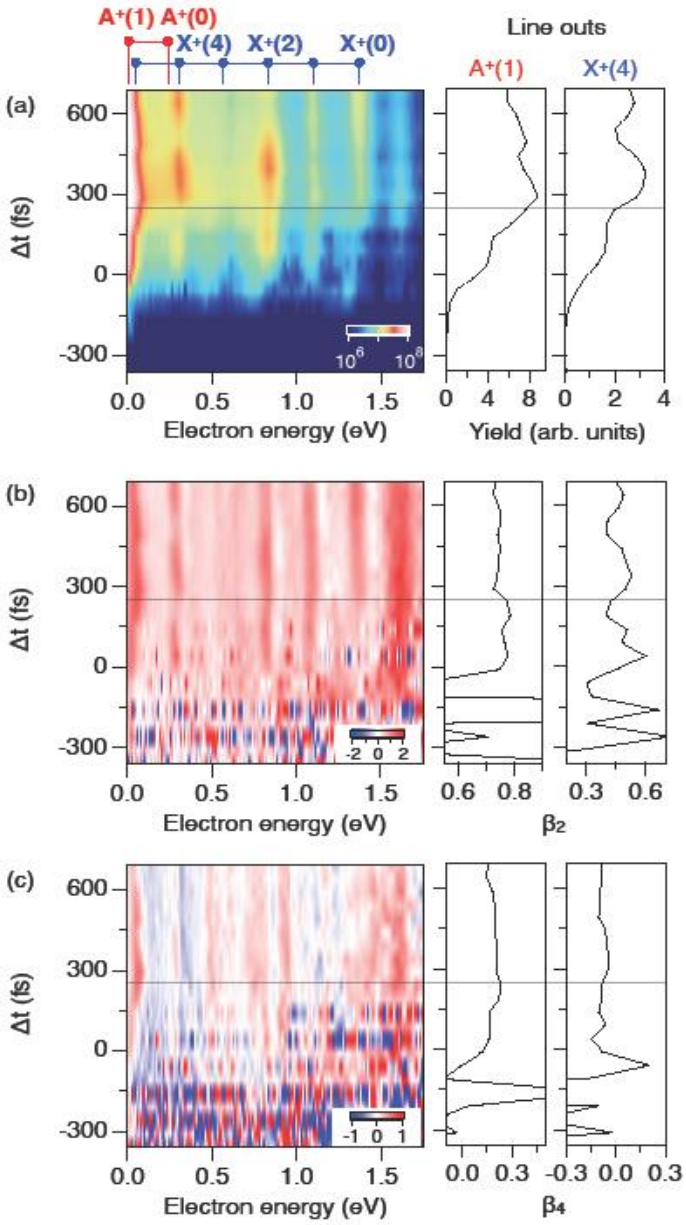

Figure 3. Two-dimensional spectrograms of photoelectron yield, and β_2 and β_4 in the region between Δt = -335 and 715 fs, for pump-control delay τ = 250 fs and phase ϕ = 0. (a) Photoelectron yield as a function of time delay (y axis) and energy (x axis, eV). The electronic final states are labelled on the top axis. (b) β_2 angular asymmetry parameter as a function of time delay and energy. (c) β_4 angular asymmetry parameter as a function of time delay and energy.

Figure 4(d) indicates that there is no change in the angular asymmetry parameter β_2, for ϕ=0, π.

Figure 4(c) shows the relative phase dependence of the X4 peak intensity at Δt = 550 fs (the position indicated by a dotted line in Fig. 4(a)). The yield is

normalized so that the signal intensity for two independent pulse excitations (i.e., no interference) is 2. When the interaction is fully coherent, the yield should vary between 0 and 4. As the pulse durations of the VUV pulses are ~140 fs (FWHM), the clear dependence on the relative phases results from molecular wave packet interference, not a trivial optical interference. The reduced contrast may be attributable to a number of factors, including decoherence effects, a non-optimal value of τ, or imperfect spatial overlap of the beams. Additional complications are discussed below. Figure 4(d) indicates that the β_2 parameter is effectively constant, and that the error of the

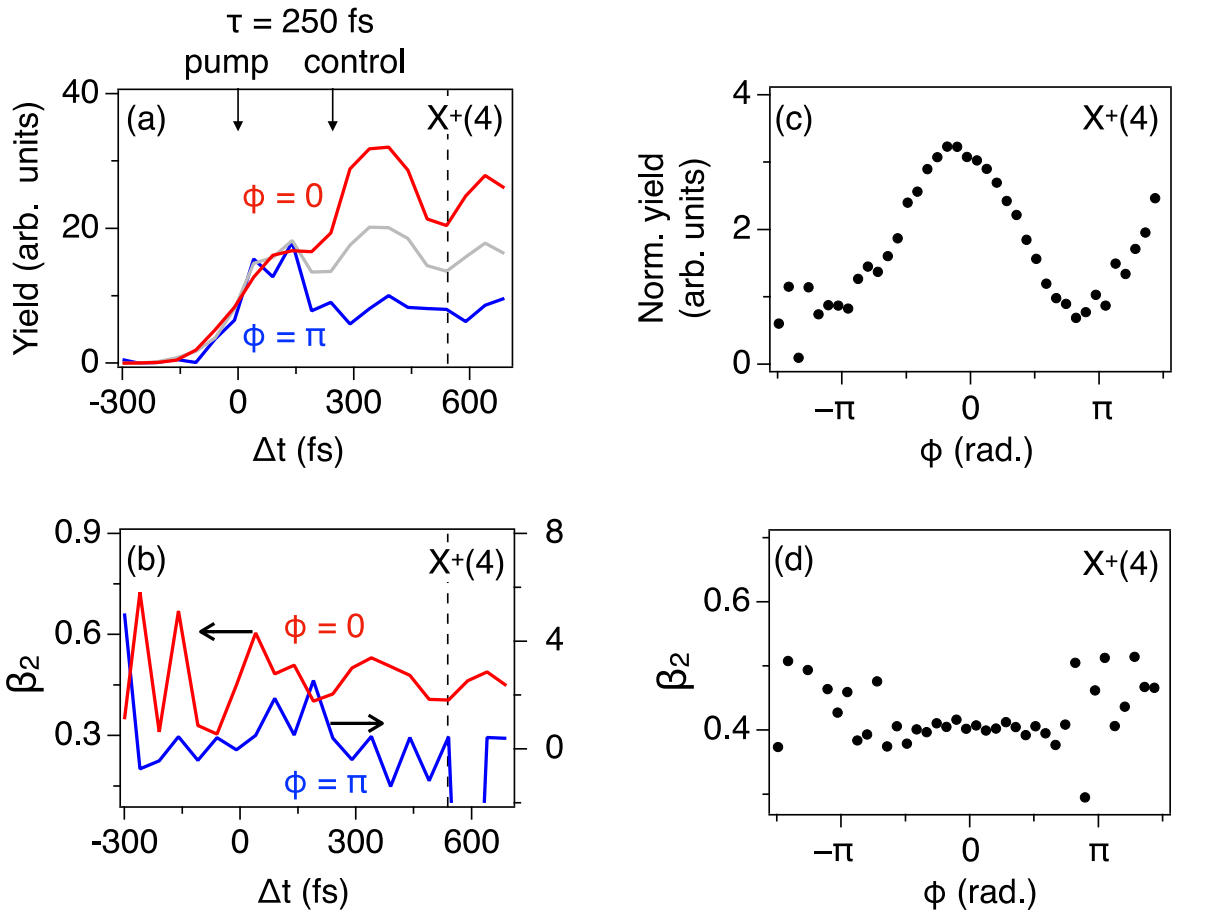

Figure 4. (a) Line outs for ϕ =0 (red), π (blue) and averaged (gray) spectrograms of the X4 state; Fig. 3(a) shows the spectrogram for ϕ =0. (b) Line outs for ϕ =0 (red) and π (blue) spectrograms of the β_2 parameter of the X4 state; Fig. 3(b) shows the spectrogram for ϕ =0. (c) Phase dependence of the X4 peak intensity at Δt = 550 fs, (dotted line in (a)). (d) Phase dependence of the β_2 parameter value Δt = 550 fs (dotted line in (b)).

measured value becomes large for values of ϕ near π and $-\pi$, where the signal is low.

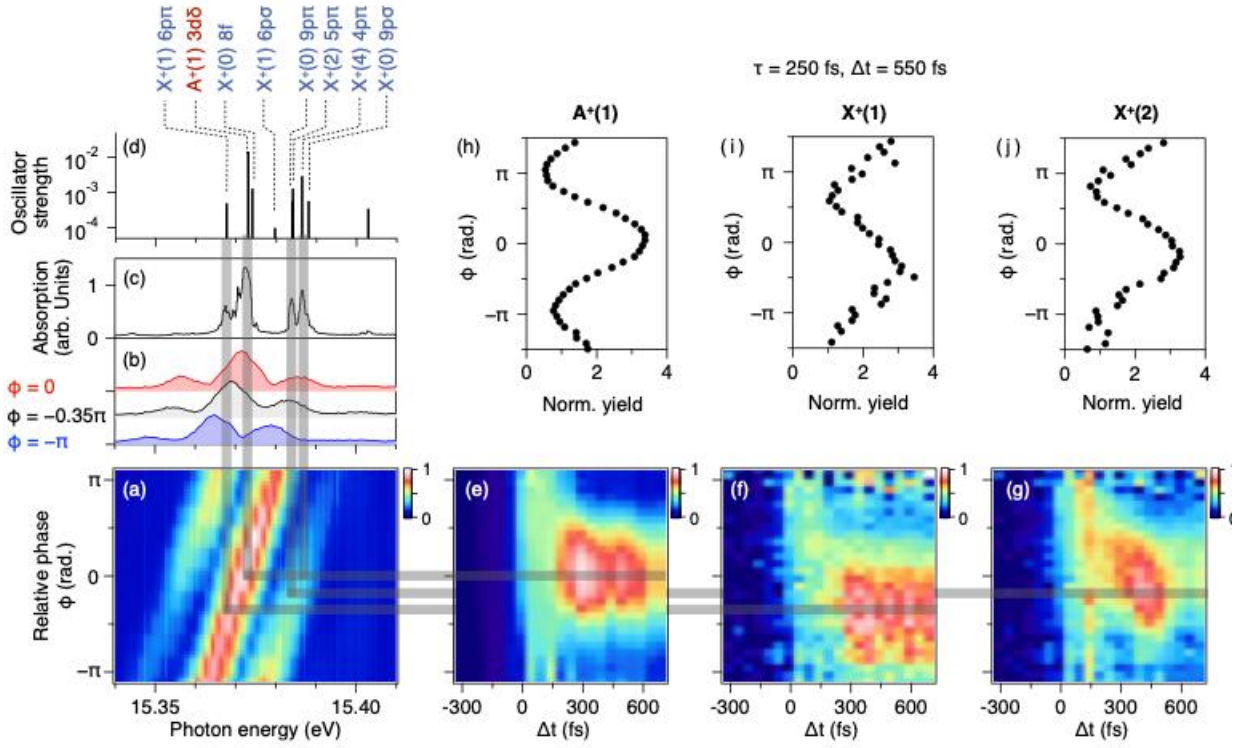

Figure 5. (a) Optical spectra of the VUV double pulses at a delay τ = 250 fs, as a function of phase. (b) Selected spectral fringe patterns for $\phi = 0$ (top, red curve), -0.35 π (middle, black), and -π (bottom, blue). (c) VUV absorption spectrum of N_2 [Ref. 32 and 33]. (d) Oscillator strengths and assignments of the transitions. (e), (f), (g) Phase dependence of the A1, X1 and A2 peaks respectively, as a function of Δt. (h), (i), (j) Line outs at Δt = 550 fs for the A1, X1 and X2 final states respectively.

Figure 5 collects and summarizes the results. Figure 5(a) shows a two-dimensional map of optical spectra, showing fringes, with line spectra at selected values of phase in Fig. 5(b), and the related absorption spectrum in Fig. 5(c). Vertical gray lines act as a guide to the eye to relate features in the spectra to the excited states. Figures 5(e), (f) and (g) show intensity maps of the A1, X1 and X2 states respectively, as a function of phase ϕ and probe delay Δt. The horizontal gray lines are a guide linking the phase values of 0 and -0.35 π of the fringe patterns with the intensity maps. Note that a maximum occurs for the A1 state at $\phi = 0$, for the X1 state at ϕ = -0.35 π, and for the X2 state at values of ϕ around -0.35 π, but depending on delay Δt. The cuts through the maps at Δt = 550 fs (where the effect is large) in Figs, 5(h), (i) and (j) show this clearly.

IV. DISCUSSION

The phase dependence of the photoelectron yield can be interpreted in terms of an overlap between the N_2 absorption spectrum and the spectral fringe pattern of a pair of VUV pulses. Figure 5(a) shows the optical spectra of the VUV double pulses, and depending on the relative phase ϕ, the spectral maxima vary continuously. The selected spectral fringe patterns for $\phi = 0$ (top), $-0.35\ \pi$ (middle), and $-\pi$ (bottom), Fig. 5(b), should be compared to the VUV absorption spectrum of N_2 [Ref. 32 and 33] shown in Fig. 5(c). The peak assignments are shown in Fig. 5(d) (as well as Fig. 1(b)) with the oscillator strengths. The spectral fringe pattern for $\phi = 0$ is optimally overlapped with the absorption peaks in Fig. 5(c) while there is a poor overlap in the case of $\phi = \pi$. When the coherence imprinted in the wave packet by the pump pulses remains until the time when the control pulse is applied, population transferred to these Rydberg states reflects the overlapped area between the absorption peaks and the spectral density of the fringe patterns.

Figure 5(e) shows the phase dependence of the A1 peak as a function of Δt. There is no phase dependence in the absence of the control pulse, which is applied at $\tau = 250$ fs. After the interaction with the control pulse, the A1 yield exhibits a sinusoidal behavior where it becomes maximum at $\phi = 0$ and minimum at $\phi = \pi$. As the A1 peak has intensity mostly coming from ionization of the A+(1)3dδ state,[25] it has maximum yield when the Rydberg state has an optimal overlap with the spectral fringe pattern for $\phi = 0$. This correspondence is identified by gray lines in Figs. 5(a)-(e).

The phase dependence of the X1 peak in Fig. 5(f) shows a similar sinusoidal behavior but with a phase shift compared to the A1 case, Fig. 5(i). This phase shift can be understood by considering how the spectral fringe pattern overlaps the absorption spectrum. The yield of the X1 peak should be proportional to population of the X+(1)6pπ Rydberg state, which is located 0.0054 eV lower than the A+(1)3dδ state.[25] Therefore, the fringe maximum is optimally overlapped with the peak position of the X+(1)6pπ Rydberg state at $\phi = -0.35\ \pi$, not $\phi = 0$, as was the case of the A1 peak.

The phase dependence of the X2 peak in Fig. 5(g) behaves in a complex manner compared to the other peaks since the phase shift continuously varies as Δt increases. The yield reflects the population of the X+(2)5pπ state which is known to mix with the A+(1)3dδ and X+(4) 4pπ states. Further experiments are required to obtain a clearer picture, but the data indicate that the initial preparation of the wave packet after the double pulse sequence of these Rydberg states strongly influences its temporal evolution, an essential aspect of this approach to control.

While the above interpretation of the present experiments in terms of the overlap of the VUV fringes with the states of interest is consistent with the present observations, it does not address some of the requirements for complete control of the ionization process. In particular, the detection of energy-resolved photoelectrons following photoionization by the IR pulse introduces some complexities that make control of the ionization process more challenging. For example, to a first approximation, Rydberg states have potentials that are nearly parallel to the corresponding potential of their ion core. Thus, ionization tends to preserve the vibrational quantum number of the core. However, there is generally some non-zero probability for producing other vibrational levels of the ion, and full vibrational state selection would require a more complex intermediate state wave packet to control these off-diagonal processes. In addition, there may be multiple components to the wave packet with significant ionization probability to a given final state. (For example, photoionization of the $X^+(0)8f$, $X^+(0)9p\pi$, and $X^+(0)9p\sigma$ states are all expected to produce the $X^+(0)$ level of the cation. See Supplementary Online information for further details). Thus, full control of the production of the $v^+ = 0$ level would require control of all three intermediate states. A third possibility is that the IR pulse could drive a core-switching transition by exciting the $X^+(v)$ of the Rydberg state to the $A^+(v')$ state rather than exciting the Rydberg electron, resulting in additional limitations on the control. Nevertheless, phase control is clearly demonstrated in Figs. 5 (e), (f), (h) and (i): by choosing a phase of φ =

0.35 π, we enhanced the excitation of the X+(1)6pπ Rydberg state, while selectively reducing the population of the A+(1)3dδ state. As is generally the case in multi-dimensional spectroscopy, additional control variables provide additional, detailed information and, in this case, we have extended the method to the VUV region. While a full map of the τ, Δt, and ϕ dependences is beyond the scope of the present effort, the results do demonstrate that controlling both the amplitudes and phases can provide significant control over the final-state photoelectron distributions.

V. CONCLUSIONS

Wave packet interferometry with two VUV pulses from the FERMI FEL has been used to control the excitation and photoionization dynamics of excited states of molecular N_2. A series of highly complex wave packets created from multiple vibronic states was prepared by these pump and control pulses. The evolution of the wave packets was monitored as a function of delay by using IR photoionization with photoelectron imaging as the detection step. This imaging detection provides both the photoelectron kinetic energy and angular distributions. In the present experiments, we demonstrate that both distributions depend on the time delay between the pump and control pulses, the relative phase of the pump and control pulses, and the subsequent delay of the IR photoionization pulse. The demonstration of this control despite the complexity of the wave packet suggests that the systematic optimization of the control parameters will allow substantial control over the final state branching ratios and angular distributions.

VI. ACKNOWLEDGEMENTS

This work was supported in part by the X-ray Free Electron Laser Utilization Research Project and the X-ray Free Electron Laser Priority Strategy Program of the Ministry of Education, Culture, Sports, Science, and Technology of Japan (MEXT) and the IMRAM program of Tohoku University, and the Dynamic Alliance for Open Innovation Bridging Human, Environment and Materials program. D.Y. acknowledges supports by JSPS KAKENHI Grant Number JP19J12870,

and a Grant-in-Aid of Tohoku University Institute for Promoting Graduate Degree Programs Division for Interdisciplinary Advanced Research and Education. We acknowledge the support of the Alexander von Humboldt Foundation (Project Tirinto), the Italian Ministry of Research Project FIRB No. RBID08CRXK and No. PRIN 2010 ERFKXL 006, the bilateral project CNR JSPS Ultrafast science with extreme ultraviolet Free Electron Lasers, and funding from the European Union Horizon 2020 research and innovation program under the Marie Sklodowska-Curie Grant Agreement No. 641789 MEDEA (Molecular Electron Dynamics investigated by IntensE Fields and Attosecond Pulses), and the RFBR and DFG for the research project No. 20-52-12023. S.T.P. is supported by the U.S. Department of Energy, Office of Science, Office of Basic Energy Sciences, Division of Chemical Sciences, Geosciences, and Biosciences under contract No. DE AC02-06CH11357. T.M. and M.M. acknowledge support by Deutsche Forschungsgemeinschaft Grant No. SFB925/A1. We thank the machine physicists of FERMI for making this experiment possible by their excellent work in providing high quality FEL light. H.I. and F.L. acknowledge funding from NSERC and FRQNT.

Data Availability Statement. The data supporting these results are available from the corresponding authors upon reasonable request.

REFERENCES

1. H. H. Fielding, Rydberg wave packets in molecules: From observation to control, Annu. Rev. Phys. Chem. **56**, 91 (2005).
2. K. Ohmori, Wave-Packet and Coherent Control Dynamics, Annu. Rev. Phys. Chem. **60**, 487 (2012).
3. D. J. Tannor, *Introduction to Quantum Mechanics, a Time-Dependent Perspective* (University Science Books, Sausalito, CA, 2007).
4. N. F. Ramsey, A molecular beam resonance method with separated oscillating fields, Phys. Rev. **78**, 695-699 (1950).
5. L. D. Noordam, D. I. Duncan, and T. F. Gallagher, Ramsey fringes in atomic Rydberg wave packets, Phys. Rev. A **45**, 4734 (1992).
6. K. Ohmori, H. Katsuki, H. Chiba, M. Honda, Y. Hagihara, K. Fujiwara, Y. Sato, and K. Ueda, Real-time observation of phase-controlled molecular wave-packet interference, Phys. Rev. Lett. **96**, 093002 (2006).
7. J. A. Cina, Wave-packet interferometry and molecular state reconstruction: spectroscopic adventures on the left-hand side of the Schrödinger equation, Ann. Rev. Phys. Chem. **59**, 319 (2008).
8. M. Fushitani, M. Bargheer, M. Gühr, and N. Schwentner, Pump–probe spectroscopy with phase-locked pulses in the condensed phase: decoherence and control of vibrational wavepackets, Phys. Chem. Chem. Phys. **7**, 3143 (2005)
9. L.-M. Koll, L. Maikowski, L. Drescher, T. Witting, and M. J. J. Vrakking, Phase-locking of time-delayed attosecond XUV pulse pairs, Opt. Express **30**, 7082 (2022).

10. L.-M. Koll, L. Maikowski, L. Drescher, M. J. J. Vrakking, and T. Witting, Experimental control of quantum-mechanical entanglement in an Attosecond Pump-Probe Experiment, Phys. Rev. Lett. **128**, 043201 (2022.)
11. L. Gulyás Oldal, P. Ye, Z. Filus, T. Csizmadia, T. Grósz, M. De Marco, Zs. Bengery, I. Seres, B. Gilicze, P. Jójárt, K. Varjú, S. Kahaly, B. Major, All-Optical Experimental Control of High-Harmonic Photon Energy, Phys. Rev. Applied **16**, L011001 (2021).
12. Andreas Wituschek, Lukas Bruder, Enrico Allaria, Ulrich Bangert, Marcel Binz, Roberto Borghes, Carlo Callegari, Giulio Cerullo, Paolo Cinquegrana, Luca Gianessi, Miltcho Danailov, Alexander Demidovich, Michele Di Fraia, Marcel Drabbels, Raimund Feifel, Tim Laarmann, Rupert Michiels, Najmeh Sadat Mirian, Marcel Mudrich, Ivaylo Nikolov, Finn H. O'Shea, Giuseppe Penco, Paolo Piseri, Oksana Plekan, Kevin Charles Prince, Andreas Przystawik, Primož Rebernik Ribič, Giuseppe Sansone, Paolo Sigalotti, Simone Spampinati, Carlo Spezzani, Richard James Squibb, Stefano Stranges, Daniel Uhl and Frank Stienkemeier, Tracking attosecond electronic coherences using phase-manipulated extreme ultraviolet pulses, Nat. Commun. **11** (2020) 883.
13. Daniel Uhl, Andreas Wituschek, Rupert Michiels, Florian Trinter, Till Jahnke, Enrico Allaria, Carlo Callegari, Miltcho Danailov, Michele Di Fraia, Oksana Plekan, Ulrich Bangert, Katrin Dulitz, Friedemann Landmesser, Moritz Michelbach, Alberto Simoncig, Michele Manfredda, Simone Spampinati, Giuseppe Penco, Richard James Squibb, Raimund Feifel, Tim Laarmann, Marcel Mudrich, Kevin C. Prince, Giulio Cerullo, Luca Giannessi, Frank Stienkemeier, and Lukas Bruder, Extreme Ultraviolet Wave Packet Interferometry of the Autoionizing HeNe Dimer, Phys. Chem. Lett. **13** (2022) 8470–8476.
14. Sergey Usenko, Andreas Przystawik, Markus Alexander Jakob, Leslie Lamberto Lazzarino, Günter Brenner, Sven Toleikis, Christian Haunhorst, Detlef Kip, and Tim Laarman, Attosecond interferometry with self-amplified spontaneous emission of a free-electron laser, Nat. Comm. **8**, 15626 (2017).

15. S. Usenko D. Schwickert, A. Przystawik, K. Baev, I. Baev, M. Braune, L. Bocklage, M. K. Czwalinna, S. Deinert, S. Düsterer, A. Hans, G. Hartmann, C. Haunhorst, M. Kuhlmann, S. Palutke, R. Röhlsberger, J. Rönsch-Schulenburg, P. Schmidt, S. Skruszewicz, S. Toleikis, J. Veifhaus, M. Martins, A, Knie, D. Kip, and T. Laarmann, Auger electron wave packet interferometry on extreme timescales with coherent soft x-rays, J. Phys. B: At. Mol. Opt. Phys. **53**, 244008 (2020).
16. Y. Hikosaka, T. Kaneyasu, M. Fujimoto, H. Iwayama and M. Katoh, Coherent control in the extreme ultraviolet and attosecond regime by synchrotron radiation. *Nat. Comm.* **10**, 4988 (2019).
17. T. Kaneyasu, Y. Hikosaka, M. Fujimoto, H. Iwayama and M. Katoh, Electron wave packet interference in atomic inner-shell excitation, Phys. Rev. Lett. **126**, 113202 (2021).
18. K. C. Prince and B. Diviacco, On "Coherent control in the extreme ultraviolet and attosecond regime by synchrotron radiation" by Hikosaka et al, Nat. Comm. **10**, 4988 (2019), Nature Communications **12**, 3784 (2021).
19. Y. Hikosaka, T. Kaneyasu, M. Fujimoto, H. Iwayama, and M. Katoh Reply to 'Comment on "Coherent control in the extreme ultraviolet and attosecond regime by synchrotron radiation"', Nature Comm. **12**, 3782 (2021).
20. R. G. Gordon and S. A. Rice, Annu. Rev. Phys. Chem. **48**, 601–641 (1997).
21. M. Fushitani, M. Bargheer, M. Gühr, H. Ibrahim and N. Schwentner, Control of chromophore-to-bath coupling by interferometry: Cl_2 vibrational wave packets in solid Ar, J. Phys. B: At. Mol. Opt. Phys. **41**, 074013 (2008). https://iopscience.iop.org/article/10.1088/0953-4075/41/7/074013/pdf
22. Heide Ibrahim, M. Héjjas, M. Fushitani, and N. Schwentner, Phase Sensitive Control of Vibronic Guest−Host Interaction: Br_2 in Ar Matrix, J. Phys. Chem. A **113**, 7439–7450 (2009). https://pubs.acs.org/doi/full/10.1021/jp900287m#

23. H. Ibrahim, M. Héjjas, and N. Schwentner, Tracing, Amplifying, and Steering Chromophore-Bath Coherences by Ultrashort Pulse Trains, Phys. Rev. Lett. **102**, 088301 (2009). https://journals.aps.org/prl/abstract/10.1103/PhysRevLett.102.088301
24. M. Fushitani, Applications of pump-probe spectroscopy, Annu. Rep. Prog. Chem., Sect. C, **104**, 272–297 (2008).
25. M. Fushitani, S. T. Pratt, D. You, S. Saito, Y. Luo, K. Ueda, H. Fujise, A. Hishikawa, H. Ibrahim, F. Légaré, P. Johnsson, J. Peschel, E. R. Simpson, A. Olofsson, J. Mauritson, P. A. Carpeggiani, P. K. Maroju, M. Moioli, D. Ertel, R. Shah, G. Sansone, T. Csizmadia, M. Dumergue, M. B. Danailov, A. Demidovich, L. Giannessi, L. Raimondi, M. Zangrando, G. De Ninno, P. R. Ribič, and K. C. Prince, Time-resolved photoelectron imaging of complex resonances in molecular nitrogen, J. Chem. Phys. **154**, 144305 (2021).
26. M. Fushitani, T. Toida, F. Légaré, and A. Hishikawa, Probing Rydberg-Rydberg interactions in N_2 by ultrafast EUV-NIR photoelectron spectroscopy, Opt. Exp. **27**, 19702 (2019).
27. V. Lyamayev, Y. Ovcharenko, R. Katzy, M. Devetta, L. Bruder, A. LaForge, M. Mudrich, U. Person, Frank Stienkemeier, M. Krikunova, T. Möller, P. Piseri, L. Avaldi, M. Coreno, P. O'Keeffe, P. Bolognesi, M. Alagia, A. Kivimäki, M. Di Fraia, N. B. Brauer, M. Drabbels, T. Mazza, S. Stranges, P. Finetti, C. Grazioli, O. Plekan, R. Richter, K. C. Prince, and C. Callegari, A modular end-station for atomic, molecular, and cluster science at the low density matter beamline of FERMI@Elettra, J. Phys. B: At. Mol. Opt. Phys. **46**, 164007 (2013).
28. D. Gauthier, P. Rebernik Ribič, G. De Ninno, E. Allaria, P. Cinquegrana, M. B. Danailov, A. Demidovich, E. Ferrari, and L. Giannessi, Generation of phase-locked pulses from a seeded free-electron laser, Phys. Rev. Lett. **116**, 024801 (2016).

29. A. T. J. B. Eppink and D. H. Parker, Velocity map imaging of ions and electrons using electrostatic lenses: Application in photoelectron and photofragment ion imaging of molecular oxygen, *Rev. Sci. Instrum.* **68**, 3477–3484 (1997)
30. C. Svetina, D. Cocco, N. Mahne, L. Raimondi, E. Ferrari and M. Zangrando, PRESTO, the on-line photon energy spectrometer at FERMI: design, features and commissioning results, J. Synchrotron Rad. **23**, 35 (2016).
31. V. Dribinski, A. Ossadtchi, V. A. Mandelshtam, and H. Reisler, Reconstruction of Abel transformable images: The Gaussian basis-set expansion Abel transform method, Rev. Sci. Instrum. **73**, 2634-2642 (2002).
32. Ch. Jungen, K. P. Huber, M. Jungen, and G. Stark, The near-threshold absorption spectrum of N_2, J. Chem. Phys. **118**, 4517-4538 (2003).
33. K. P. Huber, M.-N. Chan, G. Stark, K. Ito, and T. Matsui, N_2 band oscillator strengths at near-threshold energies, J. Chem. Phys. **131**, 084301 (2009).
34. M. Dumergue, C. Callegari, M. Di Fraia, O. Plekan, M. Danailov, L. Raimondi, M. Zangranddo, L. Giannessi, G. De Ninno, P. Rebernik Ribič, D. You, Y. Luo, S. Saito, H. Ibrahim, F. Légaré, M. Fushitani, H. Fujise, A. Hishikawa, S. T. Pratt, P. Johnsson, J. Peschel, E. R. Simpson, A. Olofsson, J. Mauritsson, P. A. Carpeggiani, G. Sansone, P. K. Maroju, M. Moioli, D. Ertel, R. Shah, T. Csizmadia, N. G. Harshitha, S. Kühn, K. Ueda, and K. C. Prince, Wavepacket manipulation in He Rydberg states, in preparation.